Role of a Strictly Conserved Active Site Tyrosine in Cofactor Genesis in the Copper Amine Oxidase from *Hansenula polymorpha*†

Jennifer L. DuBois‡ and Judith P. Klinman*

Department of Chemistry and Department of Molecular and Cell Biology, University of California, Berkeley, California 94720

Received October 5, 2005; Revised Manuscript Received December 15, 2005

ABSTRACT: The copper amine oxidases catalyze the O_2-dependent, two-electron oxidation of amines to aldehydes at an active site that contains Cu(II) and topaquinone (TPQ) cofactor. TPQ arises from the autocatalytic, post-translational oxidation of a tyrosine side chain within the same active site. The contributions of individual active site amino acids to each of these chemical processes are being delineated. Previously, using the amine oxidase from the yeast *Hansenula polymorpha* (HPAO), mutations of a strictly conserved and structurally pivotal active site tyrosine (Y305) were studied and their effects on the catalytic cycle demonstrated [Hevel, J. M., Mills, S. A., and Klinman, J. P. (1999) *Biochemistry 38*, 3683−3693]. This study examines mutations at the same position for their effects on cofactor generation. While the Y305A mutation had moderate effects on the kinetics of catalysis (2.5- and 8-fold effects on k_{cat} using ethylamine and benzylamine as substrates), the same mutation slows cofactor formation by ∼45-fold relative to that of the wild-type (WT). Additionally, the Y305A mutant forms at least two species: primarily TPQ at lower pH and a species with a blue-shifted absorbance at high pH (λ_{max} = 400 nm). The 400 nm species does not react with phenylhydrazine or ethylamine and is stable toward pH buffer exchange, long-term storage (>3 weeks), incubation at high temperatures, or incubation with reductants and colorimetric peroxide quenching reagents. A similar species accumulates appreciably even at approximately neutral pH in the Y305F mutant, despite the fact that the rate of TPQ formation is reduced only 3-fold relative to that of WT HPAO. This small impact of Y305F on the rate of biogenesis contracts with a decrease in k_{cat} (using ethylamine as the substrate) of 125-fold. The opposing effects of mutations at position 305 in biogenesis versus catalysis indicate that a single residue can be recruited for different roles during these processes.

Many enzymes are produced in a catalytically inactive form, requiring further processing or the insertion of a cofactor at their active site for reactivity. The copper amine oxidases (CAOs)[1] are examples of such post-translationally processed enzymes. The active site cofactor, 2,4,5-trihydroxyphenylalaninequinone (also known as topaquinone or TPQ), is constructed in situ by the post-translational oxidation of an active site tyrosine side chain in the vicinity of bound Cu(II) (*1*, *2*). Cofactor maturation can be observed in vitro by reconstituting the metal-free apoenzyme with Cu(II) in the presence of O_2 (*3*). Hence, Cu(II) and O_2 are sufficient for producing the cofactor, ruling out any strict requirement for chaperones or other maturation factors. CAOs were the first-discovered members of a new class of enzymes (*4*−*6*), all of which depend on side chain-derived quino cofactors with or without an accompanying metal ion. How do CAO active sites facilitate both cofactor formation and subsequent catalysis of amine oxidation?

Scheme 1: Proposed Cofactor Formation Mechanism, Including Three Ring Motions[a]

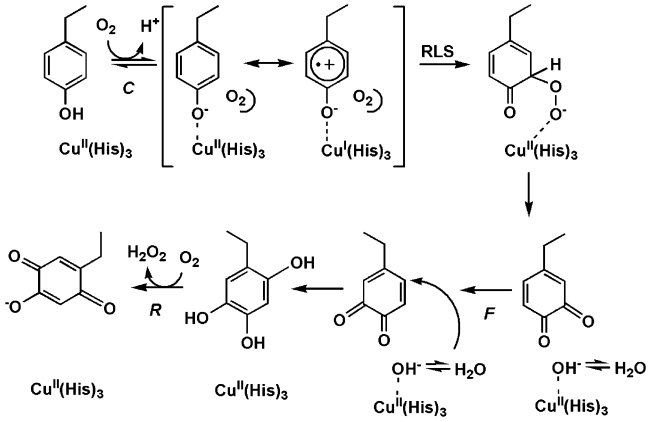

[a] RLS indicates rate-limiting step. *C*, O_2-dependent conformational change; *F*, flip; and *R*, rotation.

Chemical (*7*−*10*) and time-resolved crystallographic (*11*) data suggest a mechanism for TPQ formation (Scheme 1) in which O_2 adds to the ring C3 position of a Cu-activated tyrosine to form dopaquinone. The ring flips by ∼180°, and the C2 position is hydroxylated by a Cu(II)-bound OH^-/H_2O in a reductive Michael addition reaction. The resulting

† This work was supported by a National Institutes of Health Grant (GM 39296) to J.P.K. J.L.D. was supported by a National Institutes of Health Postdoctoral Fellowship (GM 63414).

* To whom correspondence should be addressed. Phone: (510) 642-2668. Fax: (510) 643-6232. E-mail: klinman@berkeley.edu.

‡ Present address: Department of Chemistry and Biochemistry, University of Notre Dame, Notre Dame, IN 46556.

[1] Abbreviations: CAO, copper amine oxidase; TPQ, 2,4,5-trihydroxyphenylalaninequinone; HPAO, CAO from *Hansenula polymorpha*; IPTG, isopropyl thio-β-D-galactoside. Holoenzyme refers to a protein that contains copper and TPQ.

10.1021/bi052025m CCC: $33.50
Published on Web 02/18/2006

Scheme 2: Catalytic Cycle for Copper Amine Oxidase[a]

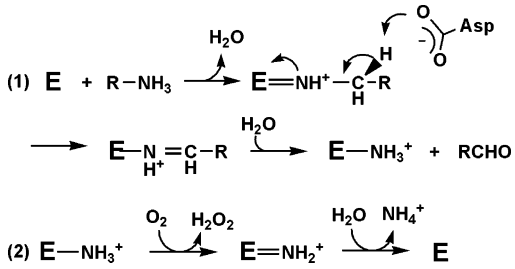

[a] (1) Reductive half-reaction and (2) oxidative half-reaction.

2,4,5-trihydroxyphenylalanine is then oxidized by O_2 to its quinone form, with concomitant production of H_2O_2, followed by rotation of the cofactor around the side chain $C_\alpha-C_\beta$ and $C_\beta-C_\gamma$ bonds into its catalytically productive conformation. As postulated by the mechanism and supported by time-resolved crystallography, cofactor formation requires at least two significant ring motions. This suggests that the active site must be sufficiently open and flexible to accommodate multiple conformations of the maturing cofactor.

The final steps in the TPQ formation mechanism are reminiscent of the oxidative half-reaction of amine catalysis by a mature, TPQ-containing enzyme (Scheme 2) (*12*). Amine oxidation begins with TPQ forming a Schiff base adduct with the amine substrate. Proton abstraction by an active site base (aspartate) drives the two-electron reduction of the cofactor and resultant two-electron oxidation of the substrate. Hydrolysis of the imine adduct yields the product aldehyde. The reduced, aminoquinol form of the cofactor is then reset for another round of the catalytic cycle by a two-electron reoxidation by O_2 to form TPQ, ammonium ion, and hydrogen peroxide.

While the cofactor maturation process requires the tyrosine ring to flip and rotate, a variety of chemical and structural data suggest that TPQ is catalytically active only when fixed in a specific conformation (Figure 1A) (*13*, *14*). This conformation has the reactive, C5 carbonyl pointing toward the active site base (Asp319), where it is optimally positioned for removal of the proton from the substrate Schiff base adduct. The C4 oxyanion is held in place by a close hydrogen bonding interaction with a strictly conserved tyrosine, residue position 305 in the amine oxidase from the yeast *Hansenula polymorpha* (HPAO) (*15*). A crystal structure of the *Escherichia coli* amine oxidase (ECAO) with the analogous residue mutated to phenylalanine (Y369F) shows TPQ not in its catalytic conformation but, rather, hydrogen bonded to a copper-bound water molecule (*16*). Thus, one role of this conserved residue appears to be to prevent migration of the cofactor oxyanion toward copper. Note that this contrasts with the obligatory complexation of the TPQ precursor (Y405) to the active metal during biogenesis (cf. Figure 1B).

Given the competing requirements for conformational flexibility during TPQ genesis and stability during catalysis, we have compared the consequences of mutations at Y305 on both processes. From the structures of the mature (*15*) and precursor (*17*) active sites (Figure 1A,B), it is apparent that Y305 is in a pivotal position and may serve a number of roles. However, prior studies of mutations at Y305 in mature HPAO (*18*) and at the analogous position in *E. coli* amine oxidase (Y369 in ECAO) (*16*) showed that this residue is apparently nonessential for amine catalysis. Because it is

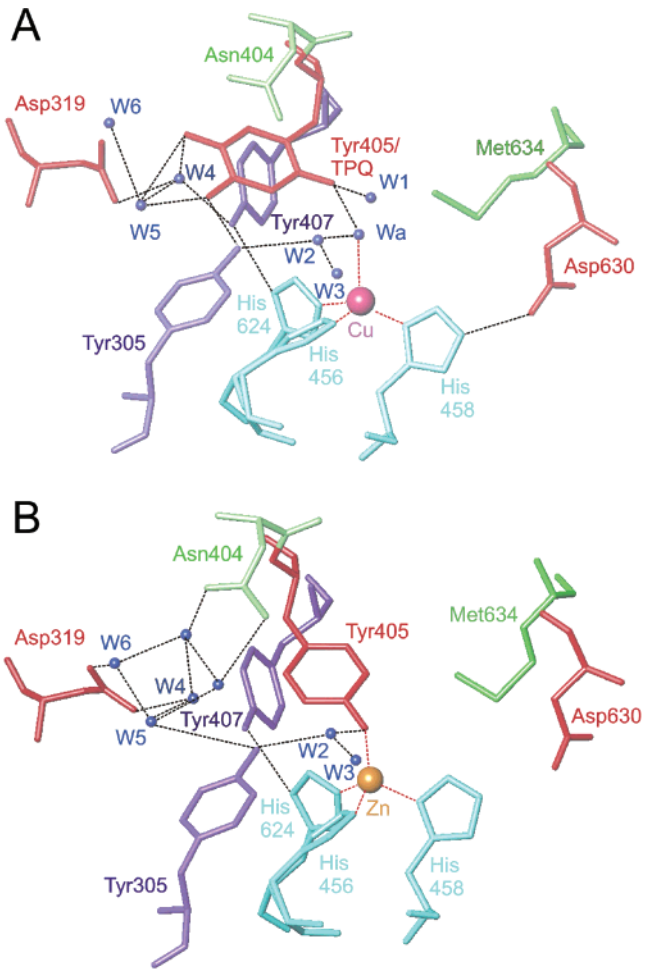

FIGURE 1: (A) Mature HPAO active site, with TPQ in the reactive conformation. Several important amino acid side chains that interact with TPQ (red) or coordinate to the Cu(II) ion (violet) are shown. The axial copper-coordinating water (Wa) and additional active site water molecules are colored blue and hydrogen bonding interactions shown (*15*). Hydrogen and metal coordination bonds are shown as black and red dashed lines, respectively. (B) Precursor HPAO active site, with Zn(II) (gold) occupying the active site and unmodified Tyr405 (red) coordinated to it. The color schemes for atoms and coordination or hydrogen bonds are the same as in panel A. All of the active site water molecules found in the mature enzyme are present in the zinc structure except W1 and Wa, which are displaced by Tyr405 in its on-copper configuration (*17*); two additional waters (unlabeled) are also bound at the vacant TPQ site.

positioned at the center of a network of active site hydrogen bonds and because it is strictly conserved, we postulated that this tyrosine might therefore serve a critical function in TPQ formation.

This study addresses the role of Y305 in cofactor production, using the same mutations previously studied in the mature enzyme (Y305F and Y305A). Several roles for Y305 are possible. Because of its proximity to the maturing cofactor, it may act as an active site base to facilitate cleavage of the C3−H bond. It could likewise act as an active site acid, donating a proton to help direct the breakdown of a ring−peroxide adduct. Beyond an overt chemical role, Y305 may serve to direct one or more of the conformational changes known to occur in the TPQ formation process. The absence of a hydrogen bond donor at Y305 may impair either a chemical or a rotational step, potentially resulting in the accumulation of intermediate species. As discussed herein, Y305 mutants exhibit complex behavior, both slowing the

rate of biogenesis in a direction opposite to catalysis [k_{BIO}(Y305F) > k_{BIO}(Y305A)] and producing a novel end product that cannot be converted to a functional TPQ. Possible structures for this product are discussed in the context of the proposed biosynthetic pathway.

EXPERIMENTAL PROCEDURES

Mutagenesis, Protein Expression, and Purification. All chemicals were of the highest available grade of purity and used without further purification. Mutagenesis of HPAO and subcloning of the mutated gene from the yeast expression vector pDB20 into the pKW3 *E. coli* expression vector were carried out as described previously (*18*). The pKW3 plasmid was transformed into electroporation-competent BL21(DE3) cells (Stratagene) for expression and storage (in 40% glycerol at −80 °C).

The growth of BL21(DE3) cells for protein expression followed previously described procedures (*19*), with some modifications. A single colony was picked from a freshly streaked plate (LB-agar, supplemented with 0.1 mg/L ampicillin), incubated for ∼10 h at 37 °C, and inoculated into 400 mL of metal-free growth medium [50% M9 salts and 50% casein (20 mg/L), where the casein has been stirred for at least 45 min with the metal chelating resin Chelex 100 (15 g/L), Sigma]. Growth medium was supplemented with 0.1 mg/L ampicillin and sterile-filtered $MgSO_4$/dextrose (50× solution, 30 mM $MgSO_4$ and 200 g/L dextrose). The 400 mL culture was grown on a shaker overnight at 37 °C and 250 rpm; 30 mL of the overnight culture was inoculated into each of 12 flasks containing 1.5 L of growth medium. Flask cultures were grown on a shaker (37 °C and 250 rpm) for ∼3 h until the cells reached an absorbance at 600 nm of 0.5−0.6. Cells were induced with 1 mM IPTG and grown for 4 h before being collected by centrifugation. Cell pellets were disrupted immediately by sonication, and the soluble portion was collected by centrifugation. Dialysis, ion exchange, and gel filtration column purification steps were carried out as previously described (*19*). Pure fractions were pooled and concentrated to ∼1.5 mL in a centrifuge filter with a 10 000 molecular weight cutoff (Millipore). Pure protein was exchanged into 50 mM HEPES buffer (pH 8) via three cycles of concentration and resuspension in 5−10 volumes of this buffer.

Mutant Y305A protein was also overexpressed in the presence of 1.2 mM ring-3,5-[$^2H_2$]tyrosine to obtain the apoenzyme incorporating the deuterated tyrosine. Cells were grown in a defined amino acid medium lacking tyrosine: each of the remaining amino acids at 0.14 g/L supplemented with 10 mL of Basal Medium Eagle (BME) vitamin solution per liter (Sigma), followed by stirring for at least 45 min with 15 g of the metal chelating resin Chelex 100 per liter (Sigma). Labeled tyrosine (Cambridge Isotopes) was added from a 2 g/30 mL (ethanol) stock at the time of induction. Protein was purified as described above.

Protein Characterization Methods. Protein concentrations were measured by the Bradford assay with bovine serum albumin as a standard (Bio-Rad Laboratories). Per-subunit copper concentrations of metal-reconstituted proteins were measured by inductively coupled plasma atomic emission spectrometry (ICP-AES, Optima 3000 DV from Perkin-Elmer), after elimination of unbound Cu(II) from the samples by buffer exchange (three cycles of dilution in 3−5 volumes of metal-free 50 mM HEPES, followed by concentration in a centrifuge microconcentrator, 10 000 molecular weight cutoff, Millipore). The degree of incorporation of ring-3,5-[$^2H_2$]tyrosine into the labeled protein was determined by quantitative liquid chromatography−tandem mass spectrometry (LC−MS/MS) on a Micromass Q-Tof hybrid quadrupole time-of-flight mass spectrometer carried out by the Stanford PAN facility. Prior to analysis, proteins (1−2 mg) were reduced, the cysteines iodoacetylated, and the proteins segmented into <4000 molecular weight peptides by proteolysis using trypsin (2 mg, 8 M urea, 37 °C, 24 h). Masses of six randomly selected tyrosine-containing peptides were analyzed by LC−MS/MS as a measure of the extent of incorporation of the label into the protein as a whole.

Cofactor Formation Kinetics. TPQ formation was monitored spectrophotometrically on an HP8452A (Hewlett-Packard) UV−visible spectrophotometer fitted to a temperature control bath. A quartz cuvette with a 100 μL fill volume was fused to a small tear drop flask with a standard 14/20, septum-sealable neck. This was used with 94−96 μL samples containing 40−60 μM apoprotein monomer (HPAO is a homodimer) in the appropriate pH buffer. Samples were spread over the surface of the flask portion of the septum-sealed cuvette and made anaerobic by a continuous purge of argon for 30−40 min at 4 °C. A 1 mM solution of $CuCl_2$ was similarly made anaerobic by continuous bubbling of argon for 20−30 min. One equivalent of the anaerobic Cu(II) was added by gastight syringe to the protein samples, and changes in the spectrum (200−700 nm) were monitored every 1−2 min for 1 h. Once the spectrum stopped changing, a t_0 spectrum was measured and the samples were opened and gently purged with compressed air for 10−15 s. Spectra were measured at 2 or 10 min intervals for 2 or 12 h (for the Y305F or Y305A mutant, respectively). Changes at particular wavelengths over time (e.g., increases at the TPQ λ_{max} = 480 nm) were fitted to single-exponential curves of the form $y = m_1(1 - e^{-kx}) + m_2$, using the Kaleidagraph program, to determine the characteristic k_{obs}.

Effect of pH on Cofactor Formation. Spectral changes during cofactor formation were monitored as a function of pH using the following buffers: 50 mM MES at pH 6.5, 50 mM HEPES at pH 7, 50 mM HEPES at pH 8, and 50 mM CHES at pH 9. Buffers were brought to the appropriate pH using KOH. For spectral end points, 60 μM samples of Y305A or Y305F proteins were incubated with 1 equiv of $CuCl_2$ in the presence of air for at least 4 days at 4 °C. Samples were exchanged into neutral pH buffer (50 mM HEPES, pH 7) by three cycles of dilution and/or resuspension, as described above. Alternatively, samples were buffer exchanged by dialysis in microdialysis cups (Millipore), with changes of the dialysis buffers every 6 h for four cycles. Samples produced by either method of buffer exchange yielded identical UV−vis spectra. Thermal incubation of samples was carried out in a water bath at temperatures ranging from 25 to 37 °C for 20−60 min, as specified.

Phenylhydrazine Assay. The amount of TPQ formed under various conditions was measured by its reaction with phenylhydrazine. Cofactor formation was carried out as described above at pH 6.5 and 9 for both Y305A and Y305F, in 100 μL samples, with 20 μM protein. Once spectral end points were reached (i.e., at $t \geq 5t_{1/2}$ for the reaction), 5 equiv

of phenylhydrazine was added to the samples from freshly prepared 100× stocks and spectral changes were monitored every 20 s at 25 or 37 °C. An absorption λ_{max} of ~440 nm was observed and monitored over time.

Steady-State Kinetics. Initial rates of substrate catalysis were measured for Y305A and Y305F reconstituted as described above at pH 6.5 or 9. Enzyme was first buffer-exchanged into 50 mM HEPES (pH 7) as described above and stored at ~10 mg/mL. Assays were carried out at 37 °C using a Clark-type electrode from Yellow Springs Instruments as a function of ethylamine concentration. Samples were equilibrated with air. Buffers and all other conditions were selected to be consistent with prior work (*18*): 100 mM potassium phosphate, 175 mM ionic strength, and pH 7 for Y305A and 65 mM potassium phosphate, pH 8, and 175 mM ionic strength for Y305F. Higher-pH buffer was used previously with Y305F to obtain faster initial rates, as measured values were otherwise near the detection limit of the O_2 electrode (*18*). Reactions were initiated by addition of 1−2 μL of enzyme to stirred solutions of gas-equilibrated buffer, and enzyme concentrations were adjusted to reflect the amount of active TPQ (as determined by reaction of TPQ with phenylhydrazine) (*20*). The initial, linear portion of each $\Delta[O_2]/\Delta t$ curve (initial ~5% of the reaction) was fit to a straight line by linear regression (Kaleidagraph). Plots of initial rate versus substrate concentration were made for Y305A and Y305F reconstituted at both extremes of pH (6.5 and 9). Curves were fit to the Michaelis−Menten equation using Kaleidagraph, yielding values for k_{cat} and k_{cat}/K_M(amine).

Tests for an Aryl-Peroxide Species. The possibility of aryl-peroxide formation at higher pHs in Y305A was investigated by incubating concentrated samples of the enzyme (60 μM) with either a soluble oxygen atom acceptor (triethylphosphene) or reducing agents (ethanethiol and $NaCNBH_4$). The enzyme solutions were made anaerobic in septum-sealed cuvettes, as described above. Ten equivalents of each reagent was added by gastight syringe from degassed concentrated stocks, and t_0 spectra were measured (300−700 nm). The samples were incubated at room temperature for >30 min and subsequently purged with air. Samples were monitored spectrophotometrically for the appearance of quinone-associated absorbance bands. No spectral changes were detected.

A direct chemical test for protein-bound peroxides was subsequently applied. The assay, using xylenol orange dye, has been described previously in studies of lipoprotein peroxidation (*21*−*23*). Briefly, samples were 25 mM H_2SO_4 (pH <2), 100 μM xylenol orange, and 100 μM Fe(II)NH_4-SO_4. Cumene hydroperoxide, used as a reference standard, was added from a fresh 1.4 mM stock to each of 11 tubes containing the ingredients described above to form 1 mL samples with final hydroperoxide concentrations from 0 to 10 μM. Samples were mixed by inversion and stored in the dark at room temperature for 30 min. Spectra were measured on an HP8452A (Hewlett-Packard) UV−visible spectrophotometer as described above. A standard curve of absorbance at 580 nm versus cumene hydroperoxide concentration was drawn and fit to a straight line with Kaleidagraph. Y305A at a concentration of 60 μM was reconstituted with Cu(II) (50 mM CHES at pH 9) and stored at 4 °C for ~48 h to reach a formation end point for the 400 nm absorbing species [$t_{1/2}$(25 °C) = 6.5 h]. Triplicate samples of protein were similarly added to the acidic xylenol orange/Fe(II) solution described above, mixed, and stored. Spectra were measured and the absorbances at 580 nm compared with the standard curve.

EPR. All spectra were measured in quartz tubes on a Bruker ER220D SRC spectrometer. For the Y305A mutant, samples were prepared at 60 μM and pH 6.5 and 9 and then concentrated to 500 μM (in a 200 μL volume) by centrifuge filtration. Spectra were measured at 7 K using a helium-cooled Oxford Instruments cryostat and instrument parameters of 9.247 GHz and 5 mW. Three scans were averaged. For wild-type HPAO, a 100 μM (protein) sample was prepared by concentrating the metal-reconstituted enzyme in pH 8 buffer, to a final volume of 200 μL. Spectra were measured at 77 K in a liquid nitrogen-cooled finger dewar with instrument parameters of 9.41 GHz and 10 mW. Seven scans were averaged. The averaged spectra were simulated using the WINEPR SimFonia software (Bruker Analytische Messtechnik GmbH) to derive values for *g* and *A*.

RESULTS

General Properties. Y305A and Y305F were expressed as apoproteins under metal-free culture conditions and subsequently reconstituted with Cu(II). Cu binding was found to be nearly stoichiometric by ICP-AES, suggesting both a low level of incorporation of specious Zn(II) during growth and maintenance of a high-affinity Cu(II) binding site in the Y305 mutants. Cu(II) binding was not affected by the pH at which the enzyme was reconstituted with Cu(II).

The metal-free apo forms of Y305A and Y305F were unstable with respect to freezing, either in cell pellets of the expression host or as purified protein. Specifically, cell pellets frozen at −20 °C and later processed for protein purification, or protein frozen rapidly in liquid N_2, did not yield spectroscopically detectable TPQ (λ_{max} ~ 480 nm) after reconstitution of the apoprotein with Cu(II). Wild-type apoprotein, by contrast, forms TPQ at unmitigated rates and stoichiometries after storage for months at −20 °C (*7*). Similarly, the Cu-reconstituted/TPQ-containing mutants, or holoproteins produced directly in the *Saccharomyces cerevisiae* expression system (*17*), showed no sensitivity to freezing. The particular sensitivity of the mutant apoproteins suggests that Y305 is important for stabilizing the active site for cofactor generation. Apoprotein mutants stored at 4 °C remained stable for 2−3 weeks, with reproducible absorbance changes upon addition of Cu (e.g., TPQ formation with λ_{max} ~ 480 nm at pH 6.5). Note that the actual λ_{max} value for Y305A, as previously reported (*17*), is slightly red-shifted to 490 nm (Table 3). However, the canonical TPQ λ_{max} of 480 nm was used for kinetics measurements (below); the TPQ λ_{max} for the mutants is therefore termed ~480 nm in this paper.

Y305A expressed in the presence of 3,5-ring-[$^2H_2$]tyrosine was trypsin-digested, and the peptides were analyzed by mass spectrometry to determine the extent of deuterium label incorporation. The masses of six different tyrosine-containing peptides were determined quantitatively by LC−MS/MS and shown uniformly to be >95% mass-shifted by 2 mass units per tyrosine, relative to the masses expected for unlabeled peptides (data not shown; cf. ref *24*). Hence, incorporation

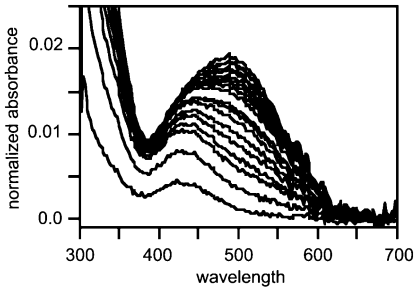

FIGURE 2: Cofactor formation reaction in Y305F at pH 6.5. The initial (t_0) spectrum has been subtracted from each subsequent spectrum to emphasize the spectral changes. (Note that the absolute magnitude of these changes is very small.) Spectra were measured every 2 min for 120 min. Data shown are for the 12 min time point and points at 12 min increments thereafter, up to 120 min.

was presumed to be nearly stoichiometric across the protein sequence.

Cofactor Formation Kinetics and Dependence on pH. The slow, single-turnover TPQ formation reaction was monitored spectrophotometrically in concentrated solutions of WT HPAO, Y305A, and Y305F. Because formation depends on Cu(II) and O_2, metal-free enzyme was first made anaerobic in a sealed UV−visible cuvette. To this was added 1 equiv of Ar-purged $CuCl_2$ by gastight syringe, and the spectral changes were monitored. As with the wild-type protein, a band at 380 nm formed immediately [within 30 s of addition of Cu(II)] and decayed slowly in a single-exponential process with rates similar to that observed in the wild-type protein (data not shown) (*7*). This absorbance has been proposed to correspond to a transient "weigh station" for Cu(II) during its migration into the active site (*7*). Because it appears as well in the Y305 mutants, the 380 nm absorbance cannot be due to a transient Y305−Cu(II)-based absorbance. Moreover, the unaltered (relative to that of the wild-type) kinetics of its appearance and disappearance suggests that the Cu binding site and metalation pathway remain intact in these mutants.

Following Cu(II) incorporation, TPQ formation is initiated by rapidly exposing the enzyme to air. For wild-type HPAO, TPQ formation occurs at a faster rate at higher pH, with a pK_a at ~8.0 (*7*). This pK_a was ascribed to the hydroxyl proton on the precursor tyrosine 405 in complex with copper. As Y305 hydrogen bonds to this hydroxyl group in the mature enzyme and may serve as an active site acid or base in TPQ formation (see below), the pH dependence of the formation reaction for Y305A and Y305F was of interest. It was thought that water molecules might be able to compensate for the absent hydroxyl group in Y305A, but not in Y305F, as the latter group is prohibitively bulky and hydrophobic. Such a hypothesis arose initially from steady-state kinetics on the mature enzyme forms of the two mutants (*18*).

The measured TPQ formation rates, however, did not follow the expected trend. At pH 6.5, Y305F forms TPQ relatively quickly (Figure 2), with a half-time ($t_{1/2}$) of 30 min (Table 1). At the same pH, Y305A forms TPQ much more slowly, with a $t_{1/2}$ of 600 min (Figure 3 and Table 1). This observed mutation dependence is the opposite of that observed in the catalytic cycle, where k_{cat}(ethylamine) is 47-fold greater for Y305A than Y305F (Table 2) (*18*).

Furthermore, the TPQ formation reaction exhibits an unexpected, pH-dependent product distribution, illustrated

Table 1: Rate Constants (min^{-1}) at 25 °C for Peak Formation during Cofactor Genesis[a]

	Y305A		Y305F		wild type
	K_{480}	k_{400}	k_{480}	k_{420}	k_{480}
pH 6.5	0.0015	ND[b]	0.027	NA[c]	0.067
pH 7	0.0025	0.0022	0.024	0.084	0.08
pH 8	0.0035	0.002	0.041	0.030	0.11
pH 9	ND[b]	0.0013	NA[d]	NA[d]	0.078[e]

[a] Values of k were determined by fitting a single-exponential curve to absorbance vs time data. Values are averages of three to five measurements. Standard deviations for all averages were ±0.002−0.005. [b] Not determined; a significant amount of the species was not observed. [c] A formation rate constant could not be determined due to significant overlap between the 420 and 480 nm bands. [d] Formation rate constants could not be measured due to protein instability under these conditions. [e] Measured at pH 8.8.

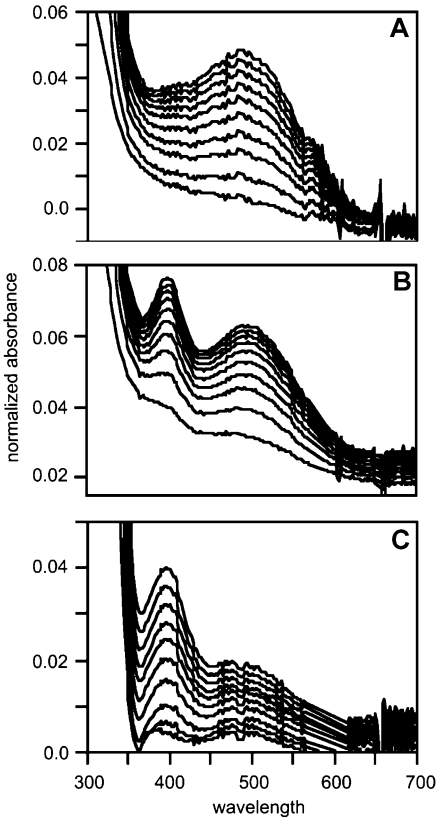

FIGURE 3: Cofactor formation in Y305A at pH 6.5 (A), 8 (B), and 9 (C). The initial (t_0) spectrum has been subtracted from each subsequent spectrum to emphasize the spectral changes. (Note that the absolute magnitude of these changes is very small.) Spectra were measured every 10 min for 12 h. For pH 6.5 and 8, data are for the 0.5 h time point and points at 0.5 h increments thereafter, up to 6 h. For pH 9, data are for the 1 h time point and points at 1 h increments thereafter, up to 12 h.

in Figure 3 for Y305A. A small shoulder at ~400 nm, adjacent to the TPQ-associated peak at 480 nm, is apparent in the end point spectrum for the Y305A cofactor formation reaction carried out at pH 6.5, in contrast to the WT enzyme that yields exclusively one end point (TPQ, $\lambda_{max} = 480$ nm). The ~400 nm peak is more prominent at pH 7 or 8 and is formed almost exclusively at pH 9. Similar spectral features are observed with cofactor formation in Y305F, except that the side peak occurs with a λ_{max} of 420 nm and is more prominent at pH 6.5 (Figure 2) than the corresponding peak at 400 nm for Y305A (Figure 3). It was not possible to

Table 2: Relative Rates of Ethylamine Oxidation for Wild-Type HPAO and Y305 Mutants Produced as Holo- and Metal-Reconstituted Proteins[a]

enzyme	k_{cat} (s^{-1})	k_{cat}/K_M (M^{-1} s^{-1})
wild-type HPAO[b]	20	5.2×10^4
Y305A holoprotein[b]	7.5	1.4×10^4
Y305F holoprotein[b,c]	0.16	0.01×10^4
Y305A reconstituted at pH 6.5	7.6	9.3×10^3
Y305A reconstituted at pH 9	10.9	4.2×10^3

[a] In 100 mM potassium phosphate at pH 7 with an ionic strength of 175 mM at 37 °C. [b] Values reported in ref *18*. [c] Rates for Y305F only were measured in 65 mM potassium phosphate at pH 8, with an ionic strength of 175 mM, and extrapolated to pH 7 using the pH curves obtained with Y305A.

measure the kinetics of peak formation at pH >8 for Y305F as the protein partially precipitated upon addition of Cu(II), disrupting the measurement. However, storage of the protein with 1 equiv of Cu(II) at 4 °C and pH 9 yielded a soluble enzyme with a spectrum very similar to the end point spectrum for Y305A, i.e., almost entirely due to the alternate species form (data not shown).

The kinetics of peak formation as a function of pH was determined for Y305F from pH 6.5 to 8 and over the full pH range of 6.5−9 for Y305A. Single-exponential curves were fit to plots of 400, 420, or 480 nm versus time to give values for k_{obs}. Averages of at least three measurements are reported in Table 1. For both mutants, k_{obs}(480 nm) appears to be maximized at pH ∼8 and k_{obs}(400 nm) or k_{obs}(420) at pH ∼7. For Y305A, values of k_{obs} at 400 and 480 nm are comparable at pH 7, with k_{obs}(400 nm) slightly less than k_{obs}(480 nm) at pH 8. At pH 9, the value for k_{obs}(400 nm) is lower still. No appreciable 480 nm species forms at pH 9.

As a control, TPQ formation was monitored optically in WT HPAO as a function of pH. In no case was a 400 nm band observed. While Y305A forms the 400 nm species up to pH 9, WT HPAO was not stable at pH >8.8. The rate of TPQ formation in WT HPAO reached a maximum at pH 8. Note that at all pHs, the rate of formation of the 480 or 400 nm species in Y305A was slower than for Y305F and 1−2 orders of magnitude slower than the observed rate constant for TPQ formation in the wild-type protein.

Stability of the Alternate Species. Spectra showing the formation of the 400 and 480 nm species in Y305A as a function of pH (Figure 3) indicate that the two species do not share an isosbestic point and do not have a precursor−product relationship. Rather, the two appear to represent distinct, pH-dependent end products for the cofactor formation process. The stability of the two species with respect to pH buffer exchange, long-term storage, and temperature was assessed. Cofactor formation was first carried out at pH 6.5 or 9, yielding primarily a band at 480 (TPQ) or 400 nm, respectively. The buffer in each of these cases was then exchanged for neutral/pH 7 HEPES (50 mM), either by cycles of dilution and filter concentration or by dialysis. In either case, the observed spectra, normalized for changes in protein concentration, were unaltered. Similarly, storing the proteins for up to 4 weeks at 4 °C did not result in any changes in the spectra, either for proteins reconstituted at the pH extrema (6.5 or 9) or for the mixture of species formed at pH 8. Thermal incubation of reconstituted proteins for up to 1 h at 40 °C and pH 6.5 or 9 had no effect on the spectra.

Reactivity with Phenylhydrazine. Phenylhydrazine reacts irreversibly with quinones, including dopaquinone, to produce brightly colored phenylhydrazone species with distinct absorption peaks for the different protonated isomers (*20*). The amount of TPQ in samples can be quantified by phenylhydrazine functionalization. Moreover, if the 400 nm species were an alternate quinone, such as the intermediate dopaquinone, it would also be expected to react with phenylhydrazine.

Attempts to quantify TPQ in samples of Y305A and Y305F by phenylhydrazine functionalization yielded mixed results. For Y305A reconstituted at pH 6.5 (and subsequently transferred to pH 7 buffer), where a 480 nm band appears to be the major spectral end product, a 440 nm band due to the TPQ−phenylhydrazine adduct forms slowly ($t_{1/2}$ = 30 min) relative to that in the wild-type (reaction complete within 5 min) with single-exponential kinetics. The 440 nm band then continues to grow, slowly, linearly, and indefinitely, over the course of >12 h (Figure 4A). Phenylhydrazine is known to oxidize slowly in air and to undergo nonspecific reactions with peptides. For the sake of quantifying TPQ, the reaction was considered complete at the end of the exponential phase, with the slight positive slope in the linear plateau region attributed to nonspecific reactions of phenylhydrazine.

Y305F does not form a single band at 440 nm after phenylhydrazine treatment under any conditions (of temperature or pH) that were tested but rather forms peaks at 360 and 440 nm that are not stable over time. Similar behavior was observed previously with mature Y305A and Y305F prepared in yeast (*18*).

The reactivity of the 400 nm end product species with phenylhydrazine was then studied. Under conditions used previously with Y305A/F holoproteins produced in vivo in yeast (10 equiv of phenylhydrazine at pH 37 °C for 30 min at pH 7), a recognizable adduct peak was not produced, possibly because of protein instability at higher temperatures. Proteins were therefore labeled under milder conditions: 2 equiv of phenylhydrazine added in 0.5 equiv increments over 2 h at 25 °C and pH 7. Under these conditions, only negligible reaction was observed with the 400 nm species formed in Y305A at pH 9 (Figure 4B). This could be attributed entirely to the small amount of TPQ in the sample, quantifying TPQ by its small 480 nm absorbance present before addition of phenylhydrazine (below).

Using [U-^{14}C]phenylhydrazine, an extinction coefficient of 25 000 M^{-1} cm^{-1} was previously determined for the phenylhydrazone adduct, and by extension, an ϵ of 1800 M^{-1} cm^{-1} was determined for TPQ in Y305A (compared to 40 500 and 2400 M^{-1} cm^{-1} in the wild-type protein, respectively) (*18*). An extinction coefficient could not be determined for Y305F in previous studies. As an approximation, the ϵ value for Y305A was used to estimate per-subunit TPQ stoichiometries for both Y305A and Y305F reconstituted at the two pH extrema (Table 3).

Reactivity with Ethylamine. Steady-state kinetic parameters for Y305A (reconstituted with Cu(II) at both pH 6.5 and 9 and then exchanged into neutral buffer) were measured for the reaction with ethylamine. Initial rate measurements for amine oxidase are typically normalized to TPQ concentration rather than enzyme concentration to reflect the percentage of enzyme containing active cofactor. The TPQ concentration

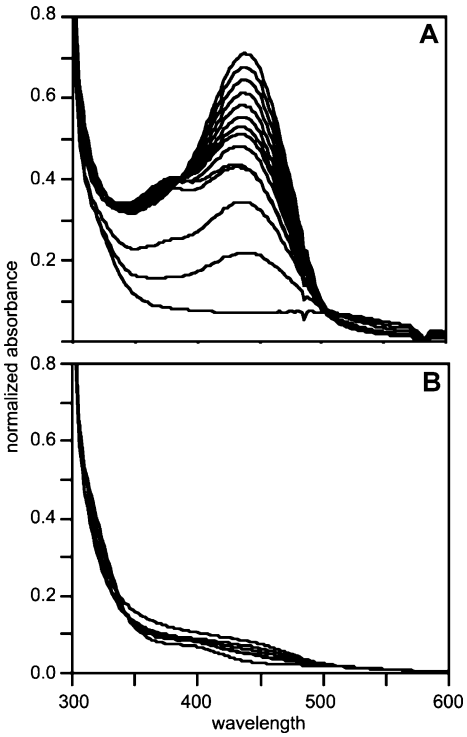

FIGURE 4: Reaction of Y305A with phenylhydrazine, when cofactor formation is carried out at pH 6.5 (A) and 9 (B). The phenylhydrazine reactions were carried out by adding 5 equiv of the hydrazine to proteins in 50 mM HEPES at pH 7 and 25 °C. The end point spectra for the experiments shown in panels A and C of Figure 3 serve as the starting spectra (t_0) for the phenylhydrazine functionalization. Spectra shown were measured at 1 min intervals after phenylhydrazine addition.

Table 3: Properties of Cofactor Formation in Y305 Mutants[a]

	Y305A		Y305F		wild type
	pH 6.5	pH 9	pH 6.5	pH 9	pH 7
% TPQ[b]	30−50	10−20	10−20	NA[c]	30−50
λ_{max} (nm)	490	400	480	420	480

[a] Listed pH values are the pH values at which the enzyme was reconstituted with 1 equiv of Cu(II). Enzyme was buffer-exchanged into 50 mM HEPES (pH 7) before the absorbance spectrum arising from titration with phenylhydrazine was recorded. [b] As determined by reaction of TPQ with phenylhydrazine at 440 nm. [c] Protein unstable at the elevated pH.

was measured for the enzyme stocks used for kinetic measurements by titration of the cofactor with 5 equiv of phenylhydrazine (at pH 7 and 25 °C), as described above. The previously measured k_{cat}/K_M for Y305A prepared as a holoenzyme from yeast (*18*) was nearly identical to the k_{cat}/K_M measured for Y305A reconstituted with Cu(II) at pH 6.5 (Table 2). Hence, these two enzyme preparations behave identically in their reactions with either phenylhydrazine or ethylamine. Y305A reconstituted with Cu(II) at pH 9 had a somewhat higher k_{cat} and a ca. 2-fold reduction in k_{cat}/K_M, relative to the enzyme reconstituted at pH 6.5.

Effect of Ring-3,5-[$^2H_2$]Tyrosine Substitution on TPQ Formation Kinetics. Y305 is well positioned to serve as a base catalyst toward cleavage of the C3−H bond in cofactor formation (Figure 1B) with a ca. 3.6 Å distance separating C3 and the Y305 hydroxyl group (*15*). In the absence of Y305, cleavage of this bond could become rate-limiting. Apo-Y305A protein was therefore expressed in minimal

Scheme 3: Possible Branching of the Transient Peroxy Derivative of Tyrosine To Form TPQ (top) or a Stable Aryl-Peroxide Intermediate (bottom)

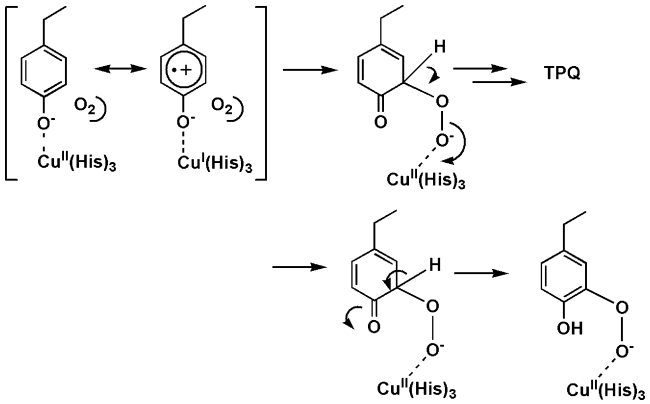

Scheme 4: Possible Roles of Y305 as a General Acid (top) or General Base (bottom) in the Breakdown of the Proposed Peroxy Derivative of Tyrosine

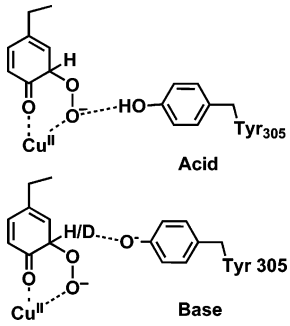

medium with an excess of ring-3,5-[$^2H_2$]tyrosine added at the time of induction, to produce a protein containing ring-3,5-[$^2H_2$]Tyr405. The kinetics of TPQ (480 nm) and side product (400 nm) formation were monitored in this protein, upon exposure of the anaerobic, Cu(II)-bound enzyme to air. No effect of protein deuteration on the formation kinetics of either species was observed. This result eliminates C3−H bond cleavage as a rate-limiting step with Y305A.

Peroxide Detection Assay. An aryl-peroxide species has been seriously considered as a candidate 400 nm species. Such a product would result from a side reaction involving rearomatization of a peroxide adduct (Scheme 3). If Y305 serves as a catalyst in directing the breakdown of this species (Scheme 4), it was plausible that mutants at Y305 would result in aberrant decomposition of this intermediate. The rearomatization of the ring species would supply a strong driving force for such an alternate pathway. However, no peroxide could be detected using high levels of protein and xylenol orange, a sensitive colorimetric reagent employed to detect other protein-bound peroxides. Additionally, attempts to reduce the peroxide using ethanethiol, $NaCNBH_4$, or the oxygen atom acceptor triethylphosphine, did not result in spectroscopically detectable quinone formation after the treated samples were exposed to air.

EPR Evidence for a Cu(II)-Ligated Species. Data that have accumulated to this point indicate that the species formed at high pH in Y305A is relatively stable and unreactive with amine substrate, phenylhydrazine, or peroxide-quenching reagents. Cu(II)-ligated TPQ is known to be unreactive or of greatly reduced reactivity, with its formation favored by

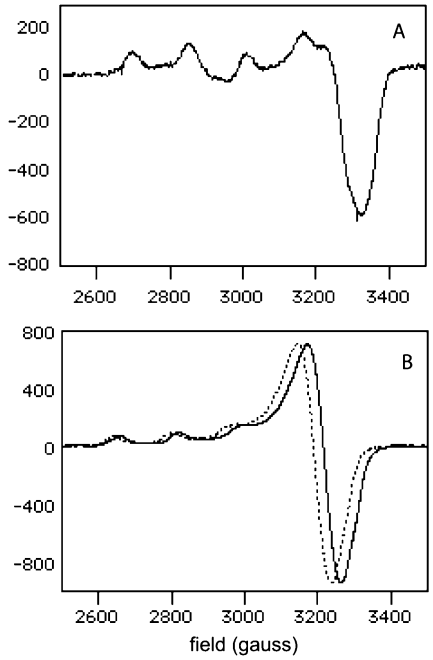

FIGURE 5: EPR spectra of WT and Y305A HPAO. (A) WT HPAO produced as a holoprotein in yeast (200 μM, 70 K). The following parameters were derived from simulations: $g_{||} = 2.295$, $g_{\perp} = 2.066$, and $A_{||} = 154$ G. (B) Y305A reconstituted with Cu(II) at pH 6.5 (—) and 9 (•••) (400 μM, 10 K). The following parameters were derived from simulations at pH 6.5: $g_{||} = 2.286$, $g_{\perp} = 2.064$, and $A_{||} = 163$ G. The following parameters were derived at pH 9: $g_{||} = 2.278$, $g_{\perp} = 2.052$, and $A_{||} = 159$ G.

certain mutations, elevated pH (presumably driven by deprotonation of the active site base), and a variety of other chemical and structural factors, not all of which are well-defined (*12*−*14*, *16*, *18*, *25*−*30*). Further, protonation of TPQ model complexes at the C4 position, or formation of a strong ion pair between the oxyanion and a counterion, has been known to strongly blue shift the absorbance of the quinone (e.g., from 480 to 380 nm) (*31*, *32*). A similar effect is seen in CAOs where the C4 oxyanion is seen ligated to Cu(II) (*27*). This raised the possibility that the species formed at high pH with the Y305 mutants was a Cu(II)-ligated TPQ or alternate Cu(II)-ligated species. This was investigated using EPR.

EPR spectra of Y305A reconstituted with Cu(II) at pH 6.5 and 9 were measured, along with spectra for wild-type HPAO (holoenzyme isolated from the *S. cerevisiae* expression system) (Figure 5). The spectrum for Y305A reconstituted at pH 6.5 yields values for $g_{\perp}$, $g_{||}$, and $A_{||}$ that are similar to those for the wild type ($g_{||} = 2.295$, $g_{\perp} = 2.066$, and $A_{||} = 154$ G) but shifted to a lower field ($g_{||} = 2.286$, $g_{\perp} = 2.064$, and $A_{||} = 163$ G). These values are shifted to yet lower fields for Y305A reconstituted at pH 9 ($g_{||} = 2.278$, $g_{\perp} = 2.052$, and $A_{||} = 159$ G). Perturbations in the observed EPR spectra suggest changes at the Cu(II) center in this mutant, reconstituted at either pH, relative to wild-type HPAO. The direction and magnitude of the observed shifts are similar to what was observed with binding of anion (N_3^-) to the Cu(II) centers in peptidylglycine α-amidating monooxygenase (*33*).

DISCUSSION

Formation of the TPQ cofactor occurs by post-translational oxidation of a tyrosine side chain at the copper amine oxidase active site. How the same active site residues facilitate this process, as well as the subsequent catalytic oxidation of amines, is the fundamental question addressed in this study.

A strictly conserved tyrosine (residue 305 in HPAO) appears to serve as a structural anchor in the mature, TPQ-containing enzyme, connecting the C4 oxyanion of the quinone to the active site Cu(II) through two hydrogen-bonded water molecules (Figure 1A) (*14*, *15*). The exceptionally close (2.4 Å) hydrogen bonding interaction between the C4 oxyanion and the Y305 hydroxyl group helps to localize negative charge at this position, stabilizing the substrate Schiff base complex formed during amine catalysis (Scheme 2). This interaction also stabilizes the proximal placement of the TPQ oxyanion and the active site base (Asp319 in HAO), preventing migration of TPQ onto Cu(II) and contributing to the relatively high pK_a (8.0) of the aspartate (*18*).

Y305 is likewise ideally situated to serve as a proton shuttle to O_2 during the oxidative half-reaction, in which two electrons and two protons are transferred from the cofactor to O_2. It almost certainly plays a role in maintaining TPQ in its reactive conformation. This proposed role is supported by the crystal structure of the equivalent of Y305F in the enzyme from *E. coli* (ECAO), Y369F (*16*). This structure shows TPQ flipped, relative to its position in active, wild-type amine oxidases, with the C4 oxyanion more closely connected to Cu(II) through a hydrogen bond to a Cu(II)-bound water molecule. In solution, the cofactor must presumably flip from this position before reaction with amine, aligning the reactive C5 carbonyl and the active site base (Asp319 in HPAO, Figure 1A).

Although Y305 is strictly conserved and positioned for several important functions during amine catalysis, mutations at this location (Y369F in ECAO and Y305A, Y305C, or Y305F in HPAO) do not abrogate catalysis. Studies of the Y369F mutant in ECAO showed a 50-fold reduction in k_{cat}/K_M(β-phenylethylamine) relative to that of the wild-type protein (*16*). The amount of TPQ in the mutant was quantified by derivatization with 2-hydrazinopyridine and shown to be roughly one TPQ per monomer. In HPAO, the Y305A substitution results in an even smaller perturbation: an ~3-fold decrease in k_{cat} and a 3.7-fold reduction in k_{cat}/K_M using ethylamine as the substrate, again with near-wild-type levels of TPQ in the enzyme as measured by reaction of the TPQ with [U-^{14}C]phenylhydrazine (*18*). This reduction in rate is, however, substrate-dependent, with k_{cat} reduced 8-fold with the poorer substrate benzylamine and k_{cat}/K_m-(benzylamine) reduced 33-fold (*18*). Though the observations are both enzyme- and substrate-dependent, it can safely be concluded that the strictly conserved active site tyrosine appears to be nonessential for catalysis of amines.

Conservation of Y305 in the CAOs could be a consequence of its essential role in TPQ formation, with three potential roles having been considered. First, Y305 could function as an active site acid, directing breakdown of a proposed aryl-peroxy-Cu(II) intermediate via protonation of the Cu(II)-proximal oxygen (Scheme 4, top). Alternatively, Y305 could serve as an active site base, facilitating the

removal of the C3 proton during breakdown of the same intermediate (Scheme 4, bottom). Finally, Y305 could serve a structural or steric role, either in facilitating the rotations known to occur during cofactor maturation (*11*) or in restricting the motion of intermediates (cf. Scheme 1).

As in prior studies of catalysis, the role of Y305 in cofactor formation was tested by mutating Y305 into either a smaller or a roughly isosteric hydrophobic, non-hydrogen-bonding side chain. The results were surprising, in that the impact was reversed in relation to that seen during catalytic turnover, showing a larger impact on the rate of cofactor formation for Ala replacement than for Phe replacement.

To further define this role and to examine possible functions of Y305 as an active site acid or base, the pH dependence of cofactor formation in Y305A was studied. As in the wild-type enzyme, cofactor formation appears to be fastest at pH 8 (Table 1) (*8*). Additionally, a new peak is observed in the absorbance spectra in the course of the cofactor-forming reaction. This peak has a blue-shifted λ_{max} (~400 nm) relative to the TPQ-associated peak with a λ_{max} of ~480 nm. The relative intensities of the novel and TPQ-associated peaks change with pH, with primarily TPQ-associated absorbance observed at lower pH (pH 6.5), two peaks observed at intermediate pH (pH 7 and 8), and largely the alternate peak at high pH (pH 9) (Figure 3). The two peaks form independently without an isosbestic point, indicating that the 400 nm species is not a direct intermediate leading to TPQ. Further, attempts to interchange the two species, e.g., by exchanging the high-pH species into low-pH buffer or vice versa, by thermal incubation of either end product (40 °C for 1 h), by long-term storage (4 weeks at 4 °C), or by incubation with reductants, resulted in no observed spectral changes. Therefore, the 400 nm species appears to be a stable alternate end product, formed preferentially at higher pH and incapable of being interconverted to TPQ.

The reactivity of the apoenzymes following reconstitution with Cu(II) at low or high pH, corresponding to an enzyme containing more TPQ or more alternate end species, respectively, was studied. Steady-state kinetic parameters were previously measured for the mutant holoproteins (Table 2) (*18*). Under the same conditions, Y305A reconstituted at low pH (i.e., appearing to contain primarily TPQ) had near-identical values for k_{cat} and k_{cat}/K_M(ethylamine). The irreversible reaction of the two different preparations of the Y305A mutant enzyme with the reagent phenylhydrazine was also studied. In either case, the reaction proceeded slowly, relative to the wild-type reaction. The extent of reaction at pH 6.5 was similar to that observed for the wild-type enzyme, with up to 40−50% of the HPAO active sites undergoing phenylhydrazone formation in the reconstituted proteins (Table 3). The low-pH end product (λ_{max} = 490 nm) is, thus, assigned to TPQ, with a slightly red-shifted absorbance (WT λ_{max} = 480 nm) due to the absence of Y305 as a strong hydrogen bonding partner (*18*).

By contrast, the alternative end product, formed by reconstitution of apo-Y305A with Cu at pH 9, reacted only sparingly with phenylhydrazine at neutral pH (Table 3). Optical (or radiometric) titration of this species at pH 7 typically showed reactivity by only ~10−20% of the enzyme. For steady-state kinetic measurements with amines, enzyme concentrations are normalized to the amount of TPQ that is available to react with phenylhydrazine. Using this convention, the k_{cat}/K_M measured for the reaction of the pH 9 species with ethylamine was reduced ~2-fold relative to the k_{cat}/K_M for the pH 6.5 species, while the k_{cat} was slightly increased (Table 2). The similar values for k_{cat} and k_{cat}/K_M suggest that the reactive species in both cases are similar, i.e., that the ethylamine reactivity is likely due to the residual 10−20% TPQ in the pH 9 enzyme and not the 400 nm species.

Given the proposed roles for Y305 in TPQ formation, it was hypothesized that the unreactive 400 nm species was an aryl-peroxide-Cu(II) charge-transfer complex (Scheme 3). If Y305 serves as an active site base in breaking the ring C3−H bond, mutants at this position could exhibit slowed, possibly rate-limiting C3−H bond cleavage. Alternatively, Y305 could serve as an acid, protonating the Cu(II)-proximal oxygen in such an intermediate and catalyzing its heterolysis. In either case, elimination of Y305 may be expected to hinder the decomposition of an initially formed, ring-peroxide adduct, leading to the accumulation of a relatively stable, aryl-peroxide species.

A series of experiments were carried out to test this proposal. First, using Y305A with ring-3,5-[$^2H_2$]tyrosine throughout its primary sequence, no kinetic isotope effect was observed for formation of either the 400 or 480 nm (TPQ) bands. Rate-limiting C3−H bond cleavage is therefore not involved in the formation of either product. This suggests that Y305 is not serving an essential role as an active site base in the decomposition of an aryl-peroxide intermediate. Resonance Raman (rR) spectroscopy was attempted unsuccessfully, as a direct probe for an aryl-peroxide; the photolability of TPQ and its presumed intermediates, as well as the tendency of highly concentrated, reconstituted protein to precipitate, has made the mutant, reconstituted protein, a difficult target for rR spectroscopy. Two chemical methods were therefore applied. Initially, reducing agents (ethanethiol and $NaCNBH_4$) and oxo-atom acceptors (triethylphosphine) were incubated with the 400 nm species in an effort to reduce the presumed aryl-peroxide species to catechol. Catechol would be expected to oxidize further to dopaquinone and subsequently to TPQ in air. However, no such production of dopaquinone or TPQ could be detected by UV−visible spectroscopy. Subsequently, a sensitive colorimetric method, based on Fe(II)-mediated disproportionation of protein-bound peroxides (*21*−*23*), was applied. Again, no peroxide species was detected using this approach.

In the absence of chemical evidence for a peroxide species, alternative options for the 400−420 nm species have been considered. In the event that Y305 is directing conformational changes during biogenesis, mutants might be expected to result in the accumulation of a misoriented TPQ that has become trapped and is unable to proceed to a functional state. The latter would be consistent with the EPR data, which indicate perturbations in the simulated parameters that show a direction and degree of change similar to what has been seen during binding of anion (N_3^-) to Cu_H in dopamine β-monooxygenase, an enzyme with a similar trihistidine Cu(II) coordination environment (*33*).

A nonproductively oriented TPQ has already been observed in a number of studies, where the C4−O^- group of the cofactor is oriented toward the copper (*12*−*14*, *16*, *18*, *25*−*30*). Additionally, bovine serum amine oxidase and several mutants of HPAO (cf., refs *30*, *34*−*36*) form stable

or semi-stable adducts with methylamine, particularly at high pH, in which the product Schiff base (PSB) form of the cofactor is proposed to rotate into an inactive conformation. Once rotated, the PSB loses its proton and remains unhydrolyzed. The absorbance for the inactive, deprotonated imine is blue-shifted (380−400 nm) relative to that of oxidized TPQ. One puzzling aspect of the data presented herein is the failure of the high-pH alternate species to react with phenylhydazine to form a detectable phenylhydrazone. In the case of the Cu-on structure seen for an ECAO mutant where the active site base was substituted with alanine, the enzyme reacted with 2-hydrazinopyridine to a small extent (*26*). A different kind of behavior was, however, seen for a nonproductively-oriented TPQ observed in the crystal structure of ECAO grown in concentrated $(NH_4)_2SO_4$ (*25*, *37*), with the enzyme remaining completely inactive even after the crystals have been redissolved. It is certainly conceivable that the inactive species detected herein are prevented from reorienting to become accessible to either phenylhydrazine or substrate under the conditions of the experiments. Though diffractable crystals have been difficult to prepare under the conditions that lead to the greatest amount of the 400−420 nm species, ongoing X-ray studies of Y305A and Y305F may elucidate the precise structural origin of the newly absorbing species and its apparent inertness to either quinone or peroxide-based reagents.

Most significantly, the data presented herein show an impact of mutations at Y305 that is the opposite of that seen during catalytic turnover. Interestingly, the bulky side chain of Y305F shows a faster rate of both cofactor and alternate product formation than Y305A. A simple kinetic model invokes the formation of an intermediate along the biosynthetic path, which partitions to a new product in the absence of the correct side chain at position 305:

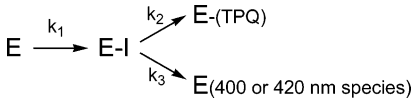

The fact that the rates of appearance of TPQ and the 400−420 nm species are similar in the case of both Y305F and Y305A suggests that the rate-limiting step for product formation resides in k_1, with the product distribution reflecting k_3/k_2. Comparison of Y305F to Y305A (Table 1) further implies that while k_1(Y305F) > k_1(Y305A), the partition ratio toward the off-pathway product is also greater for Y305F. This behavior of the Phe side chain at position 305 indicates that several factors are likely at work, for example, a role for side chain bulk in steering the formation of the E−I intermediate and a role for side hydrophobicity in skewing product formation to favor the incorrect, off-pathway species.

ACKNOWLEDGMENT

We thank Prof. Scott Mathews for his preparation of the drawings in Figure 1.

REFERENCES

1. Janes, S. M., Mu, D., Wemmer, D., Smith, A. J., Kaur, S., Maltby, D., Burlingame, A. L., and Klinman, J. P. (1990) A new redox cofactor in eukaryotic enzymes: Identification of 6-hydroxydopa at the active site of bovine serum amine oxidase, *Science 248*, 981−987.
2. Mu, D., Janes, S. M., Smith, A. J., Brown, D. E., Dooley, D. M., and Klinman, J. P. (1992) Codon identification for 6-hydroxydopa at the active site of the amine oxidase from the yeast *Hansenula polymorpha*, *J. Biol. Chem. 267*, 7979−7982.
3. Cai, D. Y., and Klinman, J. P. (1994) Evidence for a self-catalytic mechanism of 2,4,5-trihydroxyphenylalanine quinone biogenesis in yeast copper amine oxidase, *J. Biol. Chem. 269*, 32039−32042.
4. McIntire, W. S., Wemmer, D. E., Christoserdov, A. Y., and Lidstrom, M. E. (1991) A new cofactor in a prokaryotic enzyme: Tyrptophan tryptophylquinone as the redox prosthetic group of methylamine dehydrogenase, *Science 252*, 817−824.
5. Datta, S., Mori, Y., Takagi, K., Kawaguchi, K., Chen, Z.-W., Okajima, T., Kuroda, S., Ikeda, T., Kano, K., Tanizawa, K., and Mathews, F. S. (2001) Structure of a quinohemoprotein amine dehydrogenase with an uncommon redox cofactor and highly unusual crosslinking, *Proc. Natl. Acad. Sci. U.S.A. 98*, 14268−14273.
6. Wang, S., Mure, M., Medsihradszky, K. F., Burlingame, A. L., Brown, D. E., Dooley, D. M., Smith, A. J., Kagan, A. M., and Klinman, J. P. (1996) A crosslinked cofactor in lysyl oxidase: Redox function for amino acid side chains, *Science 273*, 1078−1084.
7. Dove, J. E., Schwartz, B., Williams, N. K., and Klinman, J. P. (2000) Investigation of spectroscopic intermediates during copper-binding and TPQ formation in wild-type and active-site mutants of a copper-containing amine oxidase from yeast, *Biochemistry 39*, 3690−3698.
8. Schwartz, B., Dove, J. E., and Klinman, J. P. (2000) Kinetic analysis of oxygen utilization during cofactor biogenesis in a copper-containing amine oxidase from yeast, *Biochemistry 39*, 3699−3707.
9. Schwartz, B., Olgin, A., and Klinman, J. P. (2001) The role of copper in topa quinone biogenesis and catalysis, as probed by azide inhibition of a copper amine oxidase from yeast, *Biochemistry 40*, 2954−2963.
10. Ruggiero, C. E., and Dooley, D. M. (1999) Stoichiometry of the topa quinone biogenesis reaction in copper amine oxidases, *Biochemistry 38*, 2892−2898.
11. Kim, M., Okajima, T., Kishishita, S., Yoshimura, M., Kawamori, A., Tanizawa, K., and Yamaguchi, H. (2002) X-ray snapshots of quinone cofactor biogenesis in bacterial copper amine oxidase, *Nat. Struct. Biol. 9*, 591−596.
12. Mure, M., Mills, S. A., and Klinman, J. P. (2002) Catalytic mechanism of the topa quinone containing copper amine oxidase, *Biochemistry 41*, 9269−9278.
13. Green, E. L., Nakamura, N., Dooley, D. M., Klinman, J. P., and Sanders-Loehr, J. (2002) Rates of oxygen and hydrogen exchange as indicators of TPQ cofactor orientation in amine oxidase, *Biochemistry 41*, 687−696.
14. Kumar, V., Dooley, D. M., Freeman, H. C., Guss, J. M., Harvey, I., McGuirl, M. A., Wilce, M. C. J., and Zubak, V. M. (1996) Crystal structure of a eukaryotic (pea seedling) copper-containing amine oxidase at 2.2 Å resolution, *Structure 4*, 943−955.
15. Li, R. B., Klinman, J. P., and Mathews, F. S. (1998) Crystal structure of copper amine oxidase from *Hansenula polymorpha* determined at 2.4 Å resolution, *Structure 6*, 293−307.
16. Murray, J. M., Kurtis, C. R., Tambyrajah, W., Saysell, C. G., Wilmot, C. M., Parsons, M. R., Phillips, S. E. V., Knowles, P. F., and McPherson, M. J. (2001) Conserved tyrosine-369 in the active site of *Escherichia coli* copper amine oxidase is not essential, *Biochemistry 40*, 12808−12818.
17. Chen, Z. W., Schwartz, B., Williams, N. K., Li, R. B., Klinman, J. P., and Mathews, F. S. (2000) Crystal structure at 2.5 Å resolution of zinc-substituted copper amine oxidase of *Hansenula polymorpha* expressed in *Escherichia coli*, *Biochemistry 39*, 9709−9717.
18. Hevel, J. M., Mills, S. A., and Klinman, J. P. (1999) Mutation of a strictly conserved active site residue alters substrate specificity and cofactor biogenesis in a copper amine oxidase, *Biochemistry 38*, 3683−3693.
19. Cai, D. Y., and Klinman, J. P. (1994) Copper amine oxidase: Heterologous expression, purification and characterization of an active enzyme in *Saccharomyces cerevisiae*, *Biochemistry 33*, 7647−7653.
20. Palcic, M., and Janes, S. M. (1995) Spectrophotometric detection of topa quinone, in *Redox-Active Amino Acids in Biology* (Klinman, J. P., Ed.) pp 34−38, Academic Press, San Diego.

21. Gay, C., Collins, J., and Gebicki, J. M. (1999) Hydroperoxide assay with the ferric-xylenol orange complex, *Anal. Biochem. 273*, 149−155.
22. Gay, C. A., and Gebicki, J. M. (2002) Perchloric acid enhances sensitivity and reproducibility of the ferric-xylenol orange peroxide assay. *Anal. Biochem. 304*, 42−46.
23. Gay, C. A., and Gebicki, J. A. (2003) Measurement of protein and lipid hydroperoxides in biological systems by the ferric-xylenol orange method, *Anal. Biochem. 315*, 29−35.
24. Samuels, N., and Klinman, J. P. (2005) 2,4,5-Trihydroxyphenylalanine Quinone Biogenesis in the Copper Amine Oxidase from *Hansenula polymorpha* with the Alternate Metal, Nickel, *Biochemistry 44*, 14308−14317.
25. Parsons, M. R., Convery, M. A., Wilmot, C. M., Yadav, K. D. S., Blakely, V., Corner, A. S., Philips, S. E. V., McPherson, M. J., and Knowles, P. F. (1995) Crystal structure of a quinoenzyme: Copper amine oxidase of *Escherichia coli* at 2 Å resolution, *Structure 3*, 1171−1184.
26. Wilce, M. C. J., Dooley, D. M., Freeman, H. C., Guss, J. M., Matsunami, H., McIntire, W. S., Ruggiero, C. E., Tanizawa, K., and Yamaguchi, H. (1997) Crystal structures of the copper-containing amine oxidase from *Arthrobacter globiformis* in the holo and apo forms: Implications for the biogenesis of topaquinone, *Biochemistry 36*, 16116−16133.
27. Murray, J. M., Saysell, C. G., Wilmot, C. M., Tambyrajah, W. S., Jaeger, J., Knowles, P. F., Philips, S. E. V., and McPherson, M. J. (1999) Amine oxidase: X-ray crystallographic studies with mutational variants, *Biochemistry 38*, 8217−8227.
28. Airenne, T. T., Nymalm, Y., Kidron, H., Smith, D. J., Pihlavisto, M., Salmi, M., Jalkanen, S., Johnson, M. S., and Salminen, T. A. (2005) Crystal structure of the human vascular adhesion protein-1. Unique structural features with functional implications, *Protein Sci. 14*, 1964−1974.
29. Duff, A. P., Cohen, A. E., Ellis, P. J., Kuchar, J. A., Langley, D. B., Shepard, E. M., Dooley, D. M., Freeman, H. C., and Guss, J. M. (2003) The crystal structure of *Pichia pastoris* lysyl oxidase, *Biochemistry 42*, 15148−15157.
30. Plastino, J., Green, E. L., Sanders-Loehr, J., and Klinman, J. P. (1999) An unexpected role for the active site base in cofactor orientation and flexibility in the copper amine oxidase from *Hansenula polymorpha*, *Biochemistry 38*, 8204−8216.
31. Mure, M., and Klinman, J. P. (1995) Model studies of topaquinone-dependent amine oxidases. II. characterization of reaction intermediates and mechanism, *J. Am. Chem. Soc. 117*, 8707−8718.
32. Mure, M., and Klinman, J. P. (1993) Synthesis and spectroscopic characterization of model compounds for the active site cofactor in copper amine oxidase, *J. Am. Chem. Soc. 115*, 7117−7127.
33. Chen, P., Bell, J., Eipper, B. A., and Solomon, E. I. (2004) Oxygen activation by the noncoupled binuclear copper site in peptidylglycine α-hydroxylating monooxygenase. Spectroscopic definition of the resting sites and the putative Cu^{II}_{M}-OOH intermediate, *Biochemistry 43*, 5735−5747.
34. Cai, D. Y., Dove, J., Nakamura, N., Sanders-Loehr, J., and Klinman, J. P. (1997) Mechanism-based inactivation of a yeast methylamine oxidase mutant: Implications for the functional role of the consensus sequence surrounding topa quinone, *Biochemistry 36*, 11472−11478.
35. Schwartz, B., Green, E. L., Sanders-Loehr, J., and Klinman, J. P. (1998) The relation between conserved consensus site residues and the productive conformation for TPQ cofactor in a copper-containing amino oxidase from yeast, *Biochemistry 37*, 16591−16600.
36. Nakamura, N., Moenne-Loccoz, P., Tanizawa, K., Mure, M., Suzuki, S., Klinman, J. P., and Sanders-Loehr, J. (1997) Topaquinone-dependent amine oxidases: Identification of reaction intermediates by Raman spectroscopy, *Biochemistry 36*, 11479−11486.
37. Wilmot, C. H., Murray, J. M., Alton, G., Parsons, M. R., Convery, M. A., Blakeley, V., Corner, A. S., Palcic, M. M., Knowles, P. F., McPherson, M. J., and Phillips, S. E. (1997) Catalytic mechanism of the quinoenzyme amine oxidase from *Escherichia coli*: Exploring the reductive half reaction, *Biochemistry 36*, 1608−1620.

BI052025M